



First insights into CMIP6-based hydrological projections for Central European rivers – using a small ensemble of convection-permitting climate simulations for +2 and +3 °C global warming levels

Julianna Regenauer¹, Enno Nilson¹, Claudius Fleischer¹, Caroline S. Gasten¹

5 ¹Federal Institute of Hydrology, Department M2, Koblenz, 56068, Germany

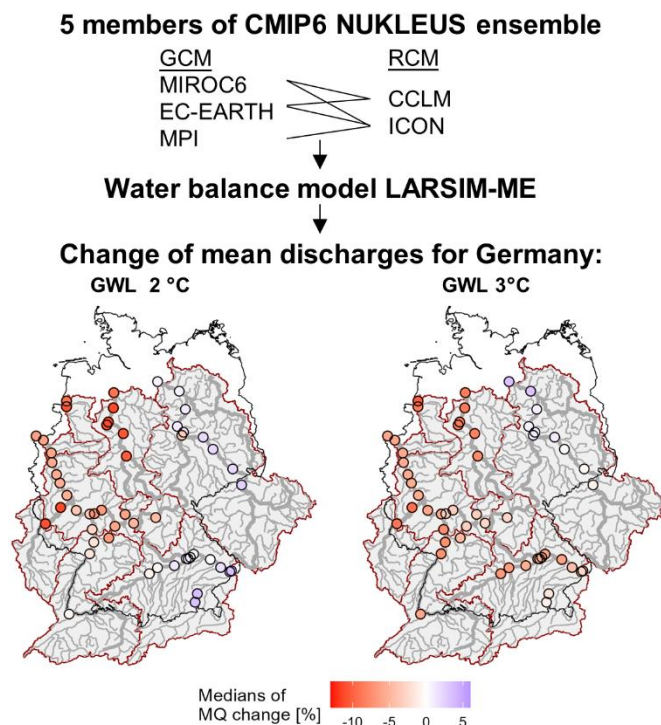
Correspondence to: Julianna Regenauer (regenauer@bafg.de)

Abstract. A warmer climate affects the hydrological regimes of rivers. It is essential to quantify these changes in order to evaluate vulnerabilities, future risks, and to develop effective adaptation strategies. To gain insights into the regional impacts of the latest generation of the Coupled Model Intercomparison Project Phase 6 (CMIP6), the NUKLEUS CMIP6 ensemble
10 (five members, three GCMs coupled to two convection-permitting RCMs) was used for first hydrological simulations for 53 German subcatchments of the Rhine, Elbe, Danube, Weser and Ems rivers with a water balance model (LARSIM-ME).

Within this preliminary ensemble, results for a 2 °C and 3 °C global warming level (GWL) show generally decreasing mean (MQ) and high flows (MHQ) in western Germany (Rhine, Weser, Ems), while in the eastern catchments (Elbe, upper Danube) high flows are projected to increase, compared to the reference period 1961–1990. Further, decreases generally display for low
15 flow indicators (MNQ) – especially for GWL 3 °C – except for heavily snow-affected catchments.

Although the results resemble features of previously observed hydrological change in those catchments (no major flood events in the Rhine River for 30 years with a MHQ decrease compared to the previous 30-years-period, very dry conditions in the last decade on a national level, significant regime changes in the Alpine region), they should be treated with caution. The east-west gradient, which manifests in the MQ and MHQ response to 2°C or 3°C warming, has not been present in discharge
20 projections of the prior CMIP5 generation. In addition, the ensemble used is comparatively small and includes two RCMs (CCLM and ICON) that are quite similar with regard to the parameterization of the precipitation processes. Nevertheless, a strong influence of the different GCMs was evident and the new phenomena of decreasing mean and high flows in western Germany could be a new climate change signal originating from the GCMs. In future analysis, change signals should be reassessed with a wider ensemble.

25



1 Introduction

Future climate projections provide an important fundament for research on climate change, its related impacts, and strategies for adaptation. The IPCC Assessment Reports rely on the Coupled Model Intercomparison Projects (CMIPs), a collaborative framework for climate modeling. CMIPs deliver current and future climate projections. These are derived from a diverse array of Global Climate Models (GCMs) developed by leading climate research institutions worldwide (Carvalho et al., 2022). Downstream activities and services at a continental and national level build upon these simulations. They thus allow for regional adaptation strategies, impact assessments and adaptation planning.

CMIP6 introduces a new generation of climate projection data that enhances our capacity to evaluate future climate scenarios. Improvements with regards to earlier generations, featuring improved resolution (Haarsma et al., 2016), a broader array of models, and more sophisticated simulations of climate processes (Carbon Brief, 2020; Try et al., 2022). Building on the basis laid by previous phases, particularly CMIP5, CMIP6 integrates advancements in climate science, computational power, and observational data (Chen et al., 2020; Eyring et al., 2016; “The CMIP6 landscape,” 2019). Each scenario of human emission in CMIP6 is constructed by combining a Representative Concentration Pathway (RCP) with a Shared Socioeconomic Pathway (SSP), as detailed in Meinshausen et al. (2020). Scenarios are named based on the SSP value followed by the RCP value. The



four chosen standard scenarios are titled as: SSP126—sustainability: taking the green road; SSP245—middle of the road; SSP370—regional rivalry: a rocky road; and SSP5.8.5—fossil-fuelled development: taking the highway (Grose et al., 2020). Regional climate models (RCMs) are used to refine the data from coarse-resolution GCMs into finer resolutions that better align with the scales used in regional impact assessments. NUKLEUS (German acronym for Useable Local Climate Information for Germany) provided an ensemble of regionally downscaled projections based on three representative GCMs, sourced from the CMIP6 generation (Laux et al., 2025). The ensemble is of temporally and spatially high-resolution and convection-permitting climate projections that provide information on climate developments at the regional and local scale (Cusinato et al., 2025). The simulations cover time slices of 30 years, including a historical period from 1961 to 1990, as well as two scenario periods representing Global Warming Levels (GWL) of +2 °C and +3 °C relative to pre-industrial conditions. These data are the first dynamically downscaled model results that have become available. A larger ensemble covering more GCMs and RCMs (EURO-CORDEX) is expected in spring 2026.

Several CMIP6 models show an Equilibrium Climate Sensitivity of 4.7 °C or more, which is significantly higher than the maximum value of the CMIP5 range of 2.1–4.7 °C (Carbon Brief, 2020). For Europe the CMIP6 ensemble on the IPCC WGI Interactive Atlas (Gutiérrez et al., 2021, available at: <https://interactive-atlas.ipcc.ch/regional-information>) shows increasing temperatures of approx. +3 °C for the mid-century and approx. +6 °C for the end of this century. Kreienkamp et al. (2020) analyzed statistical-empirical downscaled CMIP6 GCMs for Germany and compared the results to the CMIP5 generation. For SSP5-8.5, some GCMs showed temperature differences of up to +3 °C at the end-century relative to the CMIP5 scenario RCP8.5. Changes in precipitation were less distinct.

Up to now, there are only a few studies on hydrological impacts using CMIP6 projections, e.g. for Europe (Deman and Boé, 2025) and on a global scale (Wang et al., 2022; Wu et al., 2024). These studies used the GCM output without coupling to RCMs. Deman and Boé (2025) analyzed a large ensemble of CMIP6 GCMs to characterize changes in runoff for western and central Europe under SSP5-8.5 and found generally decreasing annual discharges. The same result was obtained by Wu et al. (2024) and Wang et al. (2022) for this region.

A study by Beier et al. (under review) investigating temperature and precipitation changes within the NUKLEUS CMIP6 ensemble is currently under review.

In this context, our study presents a hydrological impact modeling framework for the river catchments in Germany (Rhine, Elbe, Danube, Weser, Ems), utilizing the CMIP6 regionalization data from the NUKLEUS project. The aim is to get a more nuanced understanding of hydrological responses to climate change projections with convection-permitting models at a regional scale. By leveraging the enhanced capabilities of CMIP6, we aim to provide critical insights into the potential impacts of climate variability and change on Germany's water resources.

This leads us to the following research questions:

- Is there a significant difference in projected changes of mean flow, low flows and high flows between the two global warming levels 2 °C, 3 °C and the reference period?



- 75
- What are the differences in projected changes of mean flows between the different model combinations of the NUKLEUS CMIP6 projections?

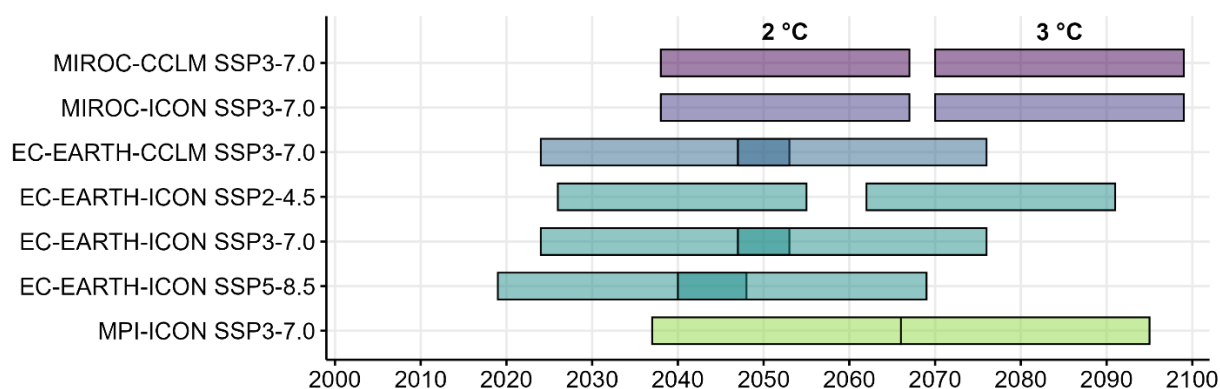
2 Data and Methods

2.1 Climate projection data

80 NUKLEUS uses three GCMs and three RCMs (nine GCM-RCM combinations). However, only the combinations listed in Fig. 1 were used for this study, as only for these five model combinations the variables precipitation, air temperature, global radiation and relative humidity were available in daily resolution at the time of download. In the NUKLEUS project the data were downscaled first to the EURO-CORDEX domain with a resolution of 12.5 km, and subsequently to an approx. 3 km resolution over Germany (and surroundings) in a convection-permitting mode (Sieck et al., 2021). The first GCM realization (r1i1p1f1) was applied for all experiments. The simulations with a resolution of 3 km and 1 hour (aggregated to daily values) cover time slices of 30 years, including a historical period from 1961 to 1990, as well as two scenario periods representing Global Warming Levels (GWL) of +2 °C and +3 °C relative to pre-industrial conditions. Since the period from 1961 to 1990 is used as a reference instead of a preindustrial time slice, it is important to note that this historical reference period corresponds to a GWL of +0.42 °C when compared to preindustrial times.

90 The GWL approach minimizes the spread of model outputs by shifting parts of the uncertainty resulting from different SSP/RCP-scenarios and climate model sensitivities while neglecting the timing of when the corresponding GWL is achieved. This approach is more compatible with current policy goals, which are also defined in terms of GWL (e.g. +1.5 °C, +2 °C). The GWL +2 °C and +3 °C (determined according to Teichmann et al. (2018)) are considered reasonable as they correspond to the critical temperature thresholds established by the Paris Agreement and current climate projections. They were also used by Rottler et al. (2021) in the Rhine catchment for analyses of flood projections. GWL +2 °C suggests a moderate level of warming suitable for near-term adaptation, whereas GWL +3 °C represents a more significant warming with long-term impacts (Laux et al., 2025). For reference, the most extreme scenario RCP8.5 in CMIP5 projected temperature increases of between 3 and 6 °C for the end of this century (Carbon Brief, 2020).

100 Five NUKLEUS GCM-RCM model combinations (see Fig.1) are used, based on two RCMs: ICON-CLM 2.6 (Van Pham et al., 2021; Zängl et al., 2015) and CCLM (COSMO-CLM 6.0, Sørland et al. (2021)). The coupling to the third RCM REMO was not used because the simulations were still ongoing and, therefore, data were not available at the time of download. The resulting ensemble encompasses runs with different SSP scenarios as shown in Figure 1.



105 **Figure 1: The applied NUKLEUS CMIP6 ensemble. The period to achieve Global Warming Levels (GWL) of +2 °C and +3 °C respectively, is shown for each applied GCM-RCM and Shared Socioeconomic Pathway (SSP) scenario. GWL 2°C and 3°C partially overlap.**

The two additional variables wind speed and air pressure, required for simulations with the water balance model LARSIM-ME, were used as a climatology (multiannual daily mean 1995-2015) of data from the high-resolution reanalysis system COSMO-REA6, since there are no suitable observation data in the reference period 1961–1990 (required for bias correction) for these variables and they are relatively insensitive for water balance modelling.

Using the Climate Data Operators (Schulzweida, 2023), the downloaded NUKLEUS climate projections were remapped on the 5 x 5 km HYRAS grid in Lambert-Conformal Conic projection via bilinear interpolation.

2.2 Bias correction

115 Due to climate model limitations, the dynamical downscaling approach does not produce an accurate representation of atmospheric variables. For hydrological impact modeling studies, a bias-correction step is advised to correct the projection data for spatio-temporal biases in the outputs of climate models before their application in hydrological modeling (Kunstmann et al., 2023). Since the bias correction done within the NUKLEUS project was not yet completed, we applied the following bias correction methods:

120 Climate projection data from the historical reference period (1961–1990) were compared to observed data (HYRAS_v5 or HYRAS_v3 for global radiation) for the corresponding period, and a correction method was estimated. With the R-package hydspatint (Klein, 2025) the Linear scaling method (additive bias correction) was applied for the air temperature (Raneesh and Thampi, 2013), and the Quantile-quantile mapping method, defined in the R-package *qmap* (Gudmundsson, 2016), was used for the parameters precipitation, global radiation and relative humidity (Boé et al., 2007; Nilson et al., 2010). In the Quantile-quantile mapping approach, values of the empirical cumulative distribution function of observed and modelled time series are derived for regularly spaced quantiles (here: 10). The bias correction parameters were estimated for each location and month of the year separately. They were then used to correct the projection data for the future periods.



The differences between corrected and uncorrected mean precipitation for the reference period show that, on average, the precipitation tends to be corrected downwards, especially in the Alps. However, a west-east gradient is also evident, which is particularly apparent in the model combinations coupled with the ICON model. Precipitation is revised upwards in the western part and downwards in the eastern part (Appendix A1). The mean temperature bias (Appendix A2) shows that air temperature is being corrected downwards, especially in the Alps for all model combination. There is hardly any difference between the coupled RCMs.

2.3 Hydrological modelling

2.3.1 About LARSIM-ME 2019

The Large area runoff simulation model (LARSIM, Bremicker (2000), LARSIM-Entwicklergemeinschaft (2024)) enables process- and area-detailed simulation and prediction of the land-based water balance. It was set up in a special configuration and parameterization for the large river basins of Central Europe relevant for Germany (model instance LARSIM-ME encompasses catchments of the rivers Rhine, Elbe, Weser, Ems and upper Danube) and further developed for climate impact analyses (Nilson et al., 2020). Hydrological processes are calculated on the basis of observed or projected future meteorological variables (precipitation, air temperature, global radiation, relative humidity, wind speed and air pressure, in daily time steps) using conceptual, physically based approximations. Water balance variables (runoff, evapotranspiration, interception, snow, groundwater recharge, etc.) are simulated on a daily time step and on a regular grid of 5 km × 5 km. Some calculation steps are carried out subscale, based on so-called land-use soil compartments or for different elevation zones within a grid cell. The interconnection of the sub-catchments, i.e., the flow direction within the model, was derived from the digital terrain model of the HydroSheds dataset v1 (Lehner et al., 2008).

2.3.2 Calibration and validation of LARSIM-ME 2019

The catchments of the stations implemented in the model determine the spatial validity range of the calibration parameters. The model was developed across all six river basins with uniform, regionalized parameter values. These regionalized parameters were calibrated in station control areas with the least possible anthropogenic influence and transferred to station control areas with similar hydrogeological properties (clusters). Selected model parameters of these regionalized model variants were subsequently fine-tuned. However, care was taken to ensure that the calibration parameters were not distorted by anthropogenic modifications to the discharge (such as dams or open-pit mines) (Wolf-Schumann et al., 2013). The calibrated catchments can be seen in Fig. 2. Calibration was performed using observation data for the period 1979–2005. The validation was carried out for the period 1951–2023 (KGE in Fig. 2) and for the same period to assess the accuracy of annual MQ, HQ and NQ (in Fig. 3).

On long stretches of the Rhine and upper Danube, good model quality measured by the Kling-Gupta efficiency (Gupta et al., 2009) is achieved (see Figure 2). At the stations of the Rhine, Elbe, Weser, Ems and upper Danube it can be described as very



160 good (frequently above 0.9, not less than 0.8). In some catchments, particularly in the areas severely impacted by anthropogenic
activities in the northeastern Elbe catchment, the model accuracy falls below 0.6. This can also be observed in a few catchments
of the upper Danube and the Rhine, which are strongly influenced by anthropogenic activities or have a relevant glacier share
(Nilson et al., 2020).

165 Figure 3 provides an overview of the sensitivity of LARSIM-ME in the individual drainage areas, using the gauging station
Kaub/Rhine as an example. Figures for four further indicator stations can be viewed in Appendix B. This shows that the model
produces good agreement with the observed discharges in the mean range, while there is a slight positive bias in the high flow
range.

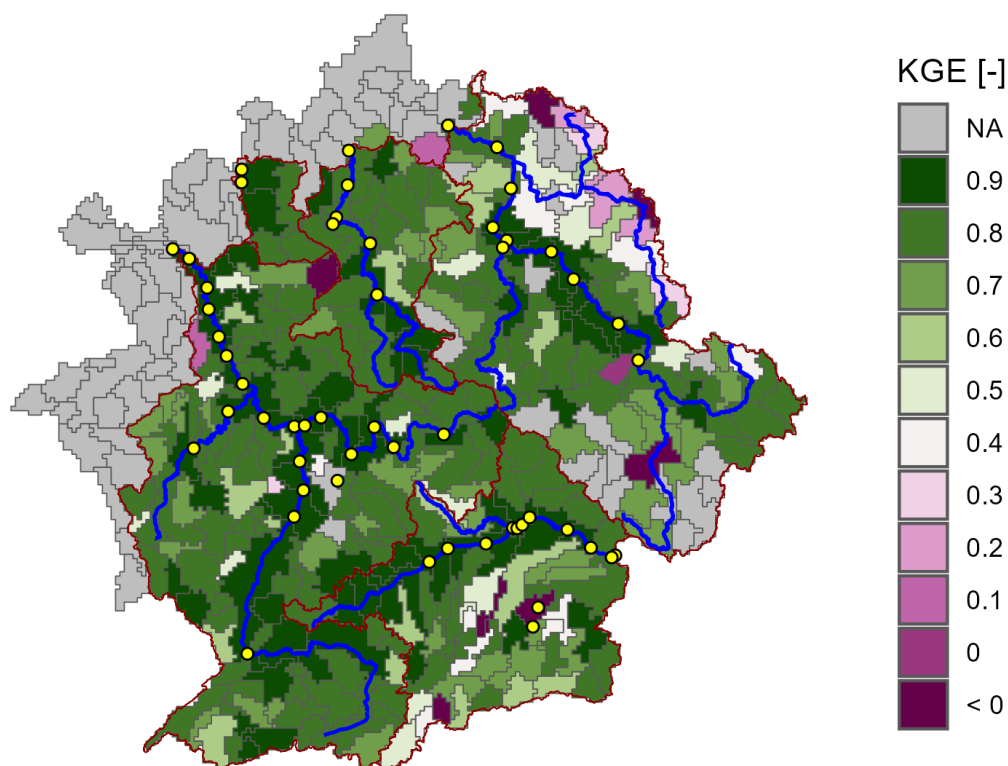
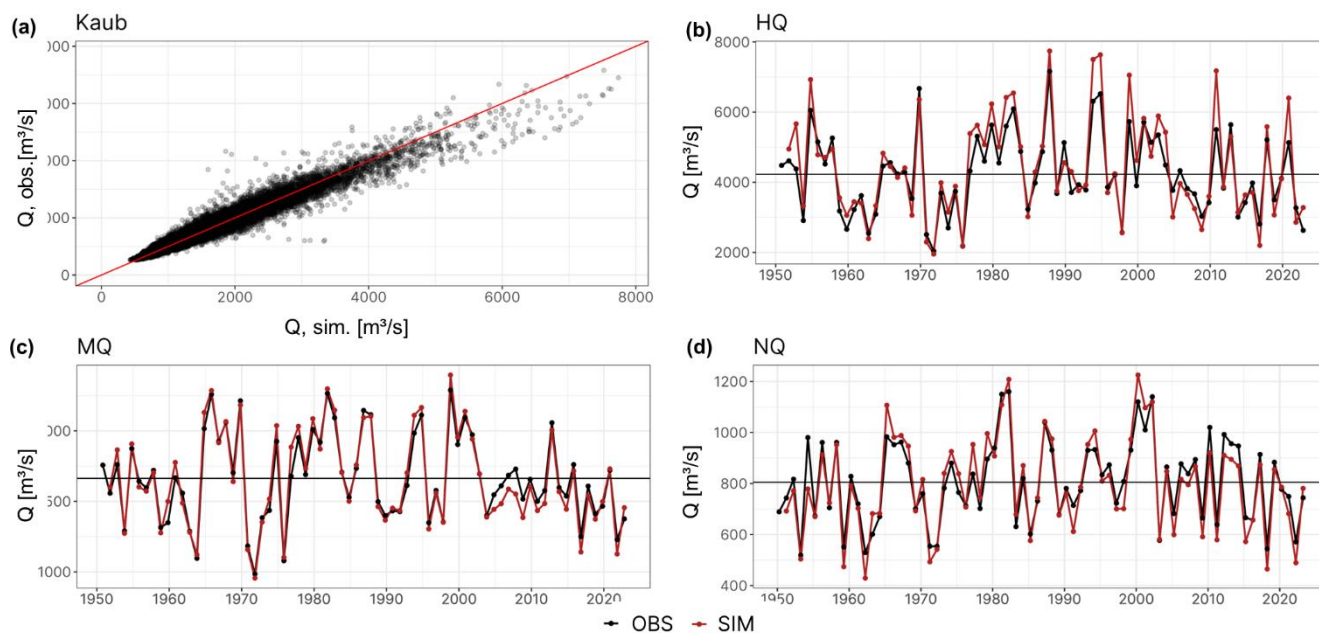


Figure 2: Model performance of LARSIM-ME 2019 model calculated using the Kling-Gupta efficiency (KGE) for the period 1951–2023 (provided observed discharge data is available) and location of 53 stations (yellow points). Grey: no observed discharge data available.



170

Figure 3: Simulated discharge (Q, sim) versus observed discharge (Q, obs) for the station Kaub/Rhine in the period 1951–2023 (a), HQ (b), MQ (c) and NQ (d).

2.3.3 Model configuration

The hydrological impact modelling was carried out with LARSIM-ME 2019 for the five river basins Rhine, upper Danube, Elbe, Weser and Ems. Detailed information on model configuration can be found in Wolf-Schumann et al. (2013) and Nilson et al. (2020).

Since CMIP6 data were only available in three 30-year-periods, each period was simulated separately. The storage capacity of a given year was used as the initial state. In order to allow the model to “warm up” and to eliminate possible artifacts of an inappropriate initial state, the first year of the simulations was not used for the following calculations of flow indicators.

180 2.4 Calculations of flow indicators

The flow indicators MQ, MHQ and MNQ (defined in more detail in Table 1) were calculated for each 29-year-period (hydrological years) or 28-year-period (water balance years) as the first year of each 30-year time period had to be discarded.

Table 1: Flow indicators calculated for all model combinations, scenarios and GWL.

Indicator	Meaning	Type of year
MQ	Mean discharge	Hydrological year
MHQ	Mean flood discharge (multiannual mean of the highest annual discharge)	Hydrological year
MNQ	Mean low-flow discharge (multiannual mean of the lowest annual discharge)	Water balance year



185 The reduced period length of only 28 years simulation periods has no major effect on the MNQ result, even for the
comparatively low MNQ values of station Dalum/Ems (approx. 0.9 % deviation, see Table C1 in Appendix C).

2.6 Study areas

To illustrate the hydrological impacts of the CMIP6 data used in this study, changes were calculated for individual catchments.
The analyses were conducted for 53 gauging stations spread across Germany, five of which serve as "indicator stations"
190 (Kaub/Rhine, Intschede/Weser, Dalum/Ems, Barby/Elbe and Hofkirchen/Danube) for each river basin (see Figure 4 and D1
in Appendix D).

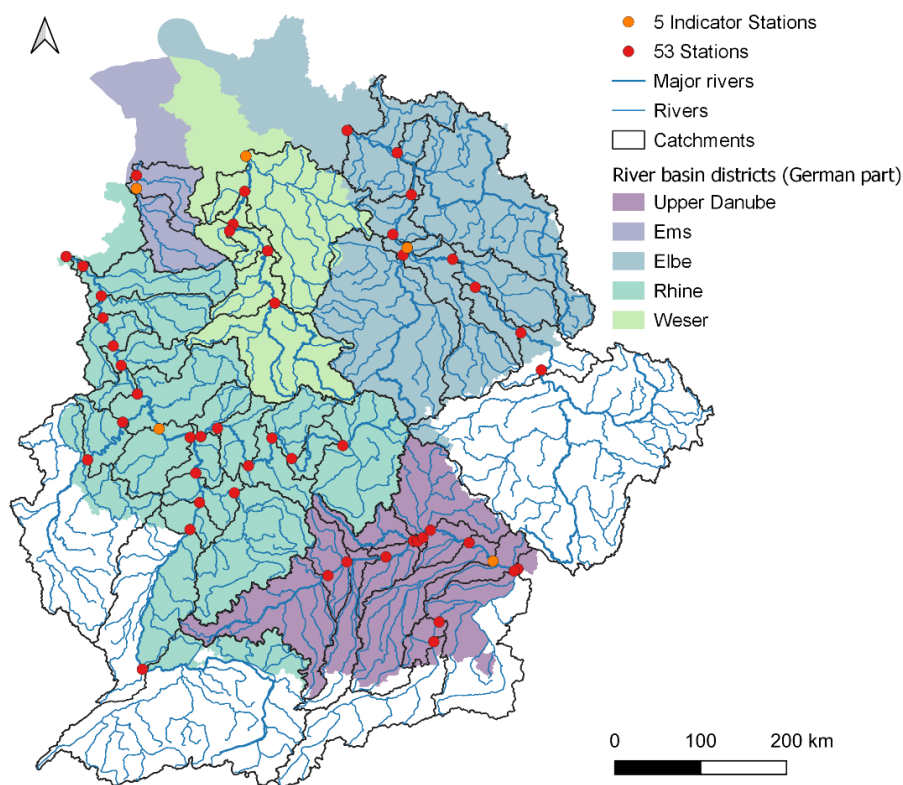


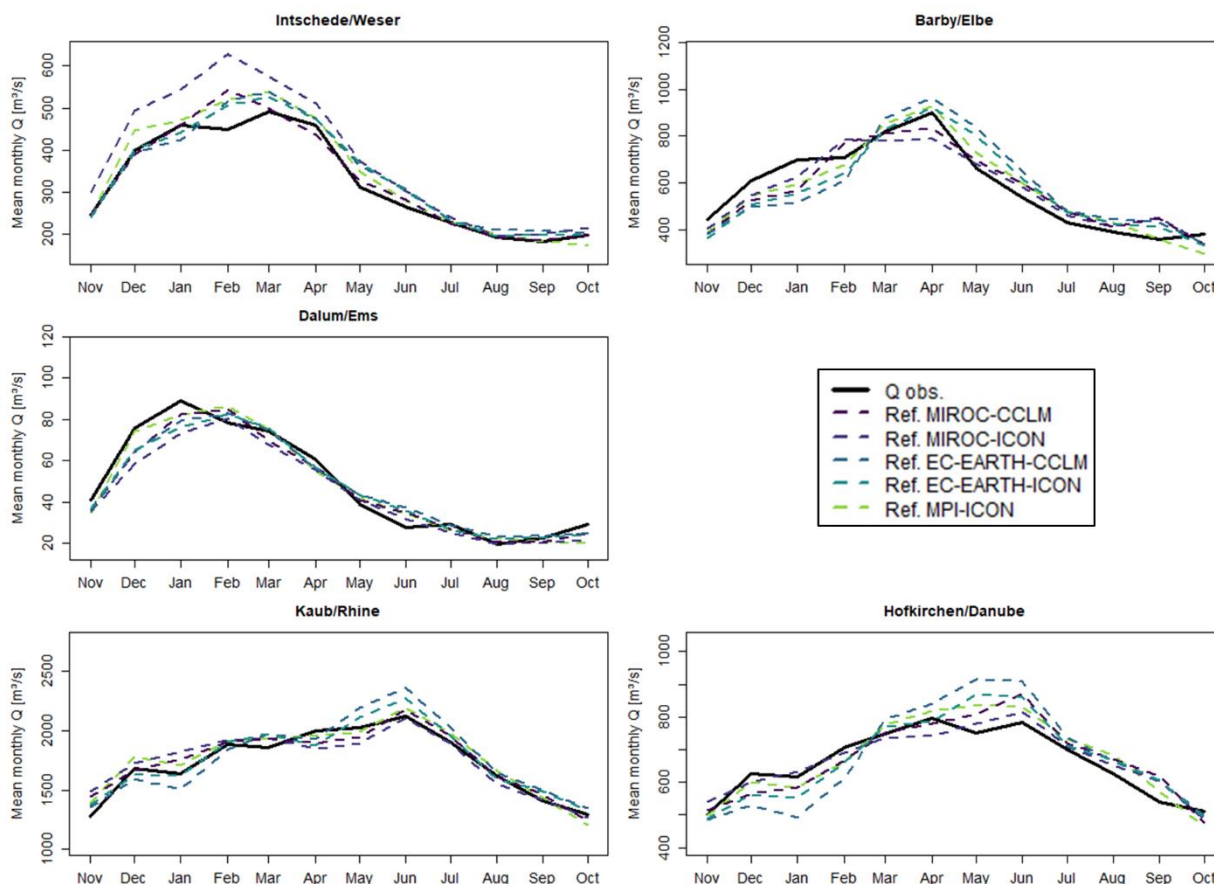
Figure 4: Evaluated catchment areas of 53 station (red) and five indicator stations (orange) in the five German river basin districts of Upper Danube, Rhine, Ems, Weser and Elbe.



195 **3 Results**

3.1 Validation of reference periods

In terms of validation of the CMIP6 reference periods the mean annual cycles of the observed discharge (Q_{obs}) and the simulated discharge for the reference periods (1962–1990) of the bias-corrected CMIP6 NUKLEUS ensemble are shown in Figure 5 for the five indicator stations.



200

Figure 5: Mean annual cycles of observed discharge (Q_{obs}) and reference periods (Ref., 1962–1990) of the five CMIP6 NUKLEUS models for the five indicator stations.

It can be stated that the simulated discharge of the reference periods closely reflect the long-term monthly average of the observed discharge at these stations. The ensemble is approximately in line with observed discharges for most months; only in winter months it is underestimated at the stations Dalum/Ems, Barby/Elbe and Hofkirchen/Danube. For February, there is an overestimation for Intschede/Weser.

205



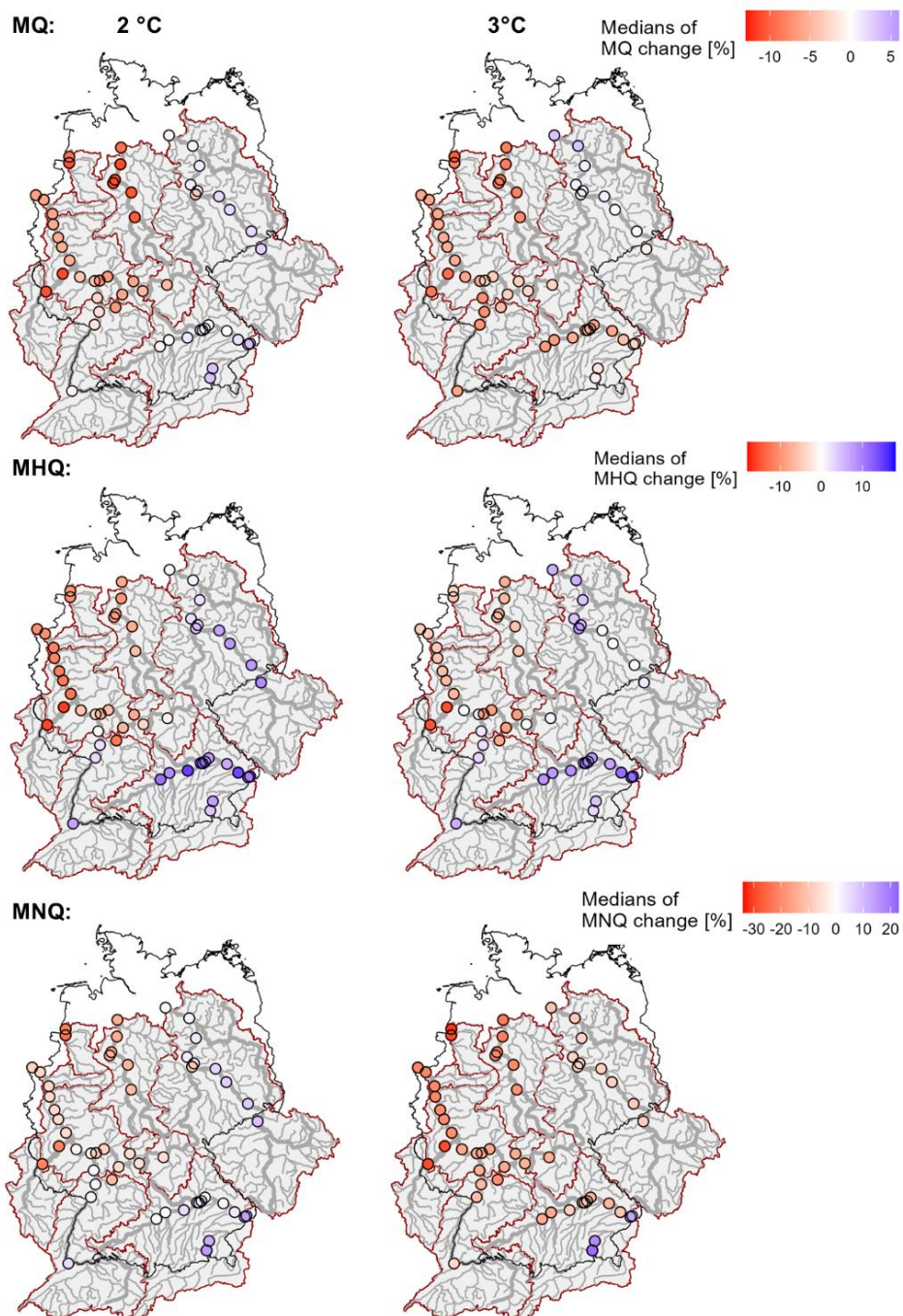
3.2 Change signal of GWL 2 °C and 3 °C for MQ, MHQ and MNQ

To investigate the development from a global warming of +2 °C to a warming of +3 °C Figure 6 shows the MQ, MHQ and MNQ changes for the NUKLEUS CMIP6 ensemble median compared to the reference period for 53 stations in Germany.

210 The NUKLEUS CMIP6 ensemble medians of MQ (top) for GWL 2 °C and GWL 3 °C show relatively similar changes: MQ decreases in the Rhine catchment (approx. -5 %, more decrease with more pluvial influences) and stronger decreases in the Weser and Ems catchments (approx. -10 %). In the eastern river basins of Elbe and upper Danube the changes are more heterogenous: no change or a slight increase for GWL 2 °C in both river basins, while for GWL 3 °C there is a slight decrease in the Danube catchment. The change of MQS and MQW (MQ in hydrological summer and winter half-year) can be seen in
215 Fig. E1 in Appendix E. This shows that the decreases in MQ are particularly drastic in summer (up to -20% in the western part of Germany).

For the high flow indicator MHQ the changes are very uniform for western river basins and eastern river basins: Slight decreases of the high flows in the Rhine catchment (again more pronounced with more pluvial regimes of the tributaries, approx. -10 %) for the 2 °C and less prominent decreases in GWL 3 °C (approx. -5 %), and similar results for the Weser and
220 Ems catchments. The river basins of Danube and Elbe, on the other hand, show rather slight increases of MHQ for both GWL (Danube: approx. +5 to +15 %, Elbe: approx. 0 to +8 %).

The low flow changes, expressed by the indicator MNQ, predominantly show decreases in the NUKLEUS CMIP6 ensemble: in GWL 3 °C for all catchments (approx. -6 to -30 %) except for those strongly influenced by snow at the Inn (+ 13 to +20 %) and Alpine Rhine. The decrease is stronger in the western catchments. For GWL 2 °C the decrease is not visible for all
225 catchments, especially the changes in the Elbe and Danube catchments are more heterogenous with no changes or slight increases.



230 **Figure 6: Flow indicators MQ (top), MHQ (center) and MNQ (bottom) for 53 catchments in the river basins of Rhine, Elbe, Danube, Weser and Ems for GWL 2 °C and 3 °C. The colors represent the changes compared to the reference period for the NUKLEUS CMIP6 ensemble median.**



3.3 Comparison of different NUKLEUS model combinations

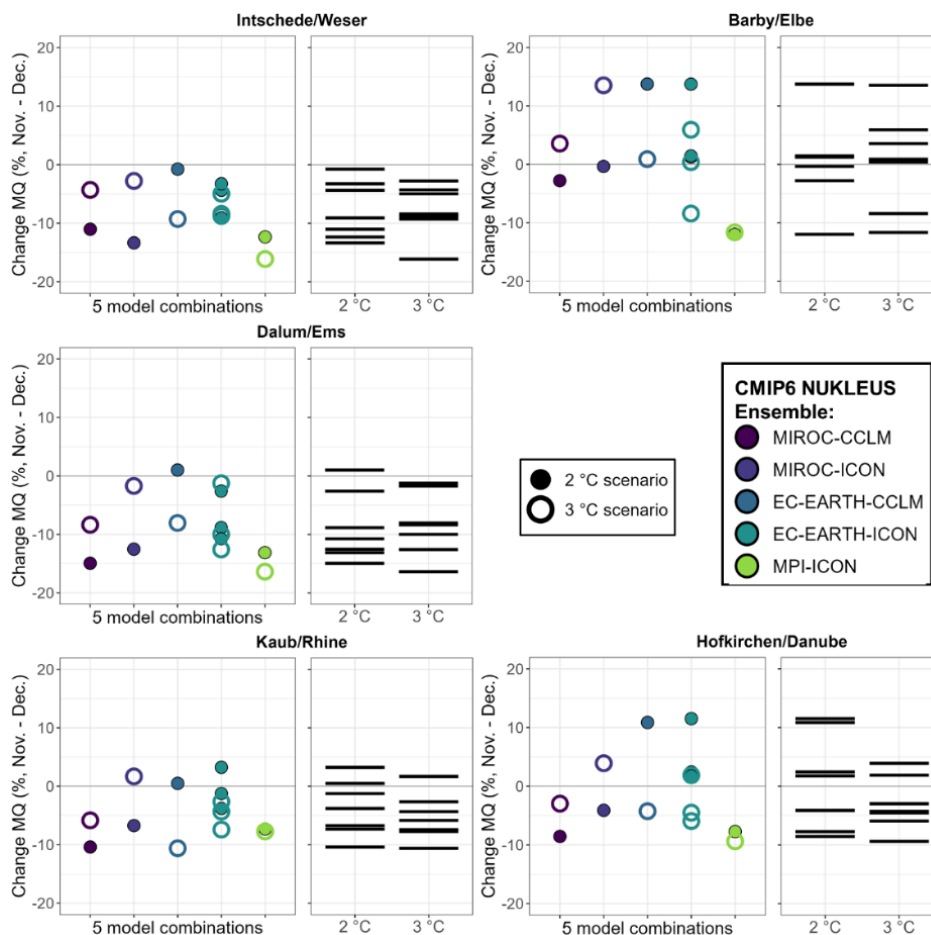
Figure 7 shows the MQ values for the five simulated CMIP6 model combinations MIROC-CCLM, MIROC-ICON, MPI-ICON, EC-EARTH-CCLM, EC-EARTH-ICON for five indicator stations in Germany (one in each river basin).

235 The colored symbols on the left represent the results of the individual model combinations and the lines on the right illustrate the entire range of all model combinations for GWL 2 °C and 3 °C, respectively.

Firstly, it is noticeable that the gauging stations in the western river basins Rhine, Ems and Weser show mostly decreasing MQ change signals (median of the ensemble), while the eastern stations in the Elbe and Danube basins do not show a clear direction of change. These differences between the eastern and western catchments were already noted in Sect. 3.2.

240 Nevertheless, the MQ values of the three western stations are very similar to each other, which also applies to the two eastern stations. The projected changes of MQ values of the western stations range from approximately -15 to 0 % (Intschede/Weser and Dalum/Ems) and from -10 to +5 % (Kaub/Rhine), with very little difference between GWL 2 °C and 3 °C. For the eastern stations, the projected change of MQ values spread from -10 to +15 % change, i.e. in a larger range. The sequence of projected MQ changes from GWL 2 °C to 3 °C of each model combination is similar for all stations and highly dependent on the driving
245 GCM: projections driven by the MIROC model show higher MQ change for GWL 3 °C than for GWL 2 °C, whereas in the EC-EARTH driven projections the MQ change of GWL 2 °C tends to be higher. The MPI model shows no significant difference between GWL 2°C and 3°C and generally has the strongest MQ decreases.

MQS and MQW (MQ for hydrological summer and winter half-year) show similar change signals between the different ensemble members and stations (Fig. F1 and F2 in Appendix F). However, for all five stations, the projected change in MQS
250 is slightly more negative than that for MQW on average. MHQ changes and MNQ changes for the individual model combinations can be found in Fig. F3 and F4 in Appendix F. Here, too, differences between the three GCMs become apparent.



255 **Figure 7: Multi-annual change signals for MQ values for five model combinations and GWL 2 °C and 3 °C of the NUKLEUS CMIP6 ensemble for five indicator stations in German river basin districts relative to 1961-1990.**

4 Discussion

Hydrological impact modeling with the new CMIP6 generation resulted in generally decreasing mean and high flows in western Germany (Rhine, Weser Ems), while in the east part (Elbe, upper Danube) high flows are predicted to increase. Further decreases were predicted for the low flow indicators.

260 The changes in the present CMIP6 discharge projections agree relatively well with some changes observed in recent decades: Floods in the Rhine catchment have been more moderate in the last 30 years, with a MHQ decrease compared to the previous 30-years period. For the nival discharge regimes of some stations in the Rhine (Basel Rheinhalles) and Danube basins (stations on the Inn), significantly different change signals (increases of MNQ, MQ and MHQ) are evident than for the more pluvial characterized catchments. In recent decades, we have seen significantly less frequent and shorter low flow events in these
 265 catchments (CIPR, 2019).



Regarding the west-east gradient in the rather decreasing (mean) discharges in western Germany and rather constant or increasing (mean) discharges in the east, a corresponding gradient in precipitation (or opposing gradient in evapotranspiration rates) can also be assumed. So far, there are few publications that focus solely on the analysis of the climate variables in the NUKLEUS CMIP6 ensemble, as the ensemble was only recently completed. But Beier et al. (under review) investigated air temperature and precipitation changes for GWL 2 °C and GWL 3 °C with respect to 1961-1990. They showed that the ensemble median for mean summer (JJA) precipitation decreases in western Germany and increases in eastern Germany for GWL 2 °C. For GWL 3 °C it generally decreases but more significantly in the west. The mean winter (DJF) precipitation shows little change (GWL 2 °C) or slight increases, especially in the south and east of Germany (GWL 3 °C). For precipitation intensity, the ensemble median increases for Germany by 7 % (GWL 2 °C) and 10 % (GWL 3 °C), with less increases in the western part and more in the eastern part. Four model combinations from the NUKLEUS CMIP6 ensemble (EC-EARTH-CCLM, EC-EARTH-ICON, MIROC-CCLM und MPI-ICON, all with SSP3-7.0) that are also included in our analysis were used and analyzed in the study of Laux et al. (2025). In terms of change in the occurrence of precipitation events, they found a west-east gradient towards more events in the eastern part of Germany and fewer events in the western part. The precipitation in the NUKLEUS CMIP6 ensemble therefore also contains a certain west-east gradient that corresponds to the resulting discharges. In contrast, the temperature increases display no gradients, but are responsible for an increase of the evapotranspiration rates which result in greater decreases of the discharges.

These findings of a gradient contradict the slightly increasing average annual precipitation of 8 % across Germany in the past (from 1881 to 2020 with respect to the average of the period 1961-1990). Although there were decreases in summer (4 %), there were increases of approx. 27% in winter, more in the western part of Germany than in the eastern part (Kaspar and Mächel, 2023). However, precipitation trends for Germany are generally relatively uncertain in climate projections, as Germany is in a transition zone between increasing and decreasing precipitation trends in Central Europe, at least for projections of the summer (Anders et al., 2014). The extent to which the novel coupling of GCM to convection-permitting RCM could be responsible for the emergence of a west-east gradient should be further investigated. In principle, precipitation and rainstorm events can be adequately reproduced in the convection-permitting RCMs (Hundhausen et al., 2025).

Especially in the model combinations coupled with ICON, there appears to be a west-east gradient in precipitation, since the bias correction in these model combinations tended to correct the western part upwards and the eastern part downwards. The bias correction method used for precipitation (Quantile-quantile Mapping), as a relative complex procedure (with estimation of 10 quantiles), is well suited for correcting precipitation, as both mean values and extremes are taken into account. However, bias correction assumes a stationarity of bias that can be hardly justified. Furthermore, Padulano et al. (2025) demonstrated that a bias at different moments in the distribution influences the preservation of the climate signal. Additionally, this preservation is affected by the signal's magnitude and the alignment between the bias direction and the signal (under- or overestimation, increase or decrease)



In contrast to the change-gradient in mean discharges in our study, the prior CMIP generation (CMIP5) projected hardly any
300 changes in mean annual discharges. Increases in high flows were generally expected for all of Germany. However, the changes
were calculated compared to other reference periods. For example, the ICPR report (2024) anticipated increases in the MHQ
for the Rhine below Maxau (reference period: 1981–2010). Based on CMIP5 simulations, the BMVI network of experts (2020)
also project more intense high and low flow situations for the end of the century in Germany (reference period 1971–2000).
A substantial difference between CMIP6 and CMIP5 is, that in many cases (Kreienkamp et al., 2020; Palmer et al., 2021)
305 central Europe is found to show a significant increase in temperature projections for CMIP6. Lower discharges could therefore
be explained by increased evapotranspiration rates. Comparisons of the CMIP6 evaluations in the present study regarding
CMIP5-based hydrological changes can only be made very roughly, since different time periods, reference periods and GWLs
are compared using the specified GWLs in the CMIP6 projections.

A potential explanation for the stronger changes in discharge patterns as part of the present analysis, may be the relatively
310 small model ensemble used within the present study (three GCM combined with two RCM) and the use of the two RCMs
ICON and CCLM which are quite similar with regard to the parameterizations of the precipitation processes. Due to the limited
bandwidth of the ensemble, the uncertainty can only be estimated with insufficient accuracy. Further uncertainties arising from
the choice of the hydrological model cannot be determined, as simulations were performed using only one hydrological model
(LARSIM-ME). An important difference to the CMIP5-based studies lies in the use of convection-permitting RCMs, whereas
315 the RCMs in the CMIP5 ensemble were not yet convection-permitting.

The analysis of Deman and Boé (2025) about the hydrological behavior of a CMIP6 GCM ensemble (36 models, SSP5-8.5)
over western and central Europe showed a general decrease in annual discharges for half of the model clusters. The other half
exhibited no significant change or a slight increase in annual discharges. They also found that the changes in precipitation and
evapotranspiration that influence these factors can differ significantly, even in terms of sign. However, the three GCMs used
320 in the present study belong to three clusters of the study (Deman and Boé, 2025) that generally predict decreasing annual
discharges with different signs of precipitation (MIROC: no change, MPI: decrease, EC-EARTH: increase) and
evapotranspiration (MIROC: increase, MPI: no change, EC-EARTH: increase). Wu et al. (2024) also calculated mean annual
discharge decreases for Europe in the long term (2080–2099) using a CMIP6 ensemble with SSP5-8.5. Resulting
evapotranspiration sums rather increase in the annual mean (because of large increases during winter). Changes in precipitation
325 are uncertain on an annual average and differ between northeast (rather increasing) and southwest (rather decreasing) of
Europe.

A clear influence of the GCM is evident, as bigger differences are found between the MQ, MHQ and MNQ changes of the
three GCMs than between the two RCMs used. The fact that the choice of the driving GCM influences the simulations more
than that of the RCM is a relatively well-known effect (Dobler et al., 2023) and was also found in the NUKLEUS data itself
330 (Beier et al., under review). This fact would suggest that the resulting changes in decreasing discharges in western Germany
could be a new climate signal originating from the CMIP6 GCMs. However, these results come from a relatively small



ensemble and are therefore subject to high uncertainties. Further investigations with the larger CMIP6-EURO-CORDEX ensemble are essential.

5 Conclusions

335 Hydrological impact modeling with the new CMIP generation (CMIP6) using regional downscaled and convection-permitting projection data from the NUKLEUS CMIP6 ensemble showed interesting developments in projected change signals of mean and high flows for a 2 °C and 3 °C warming in Germany.

New developments compared to the CMIP5 generation are primarily characterized by generally decreasing mean and high flows in western Germany, while in the eastern part high flows are still predicted to increase (as with CMIP5). Further 340 decreases were predicted for the low flow indicators – especially for GWL 3 °C – except in the Inn catchment, which is heavily affected by snow.

The ensemble used, consisting of 3 GCMs and 2 RCMs, is comparatively small and includes two RCMs (CCLM and ICON) that are quite similar with regard to the parameterization of the precipitation processes. These early results from regional CMIP6 simulations in Germany should therefore be treated with caution. More insight into the uncertainties of these results 345 will only be possible through simulations with a wide range of different models.

However, a strong influence of the different GCMs was evident: Their change signals were only slightly modulated by the two different RCMs. Therefore, the question remains whether the new phenomena of decreasing mean and high flows in western Germany could also be a new climate change signal originating from the GCMs. Further simulations with the CMIP6 EURO-CORDEX ensemble, expected in spring 2026, will clarify this.



350 Appendix A

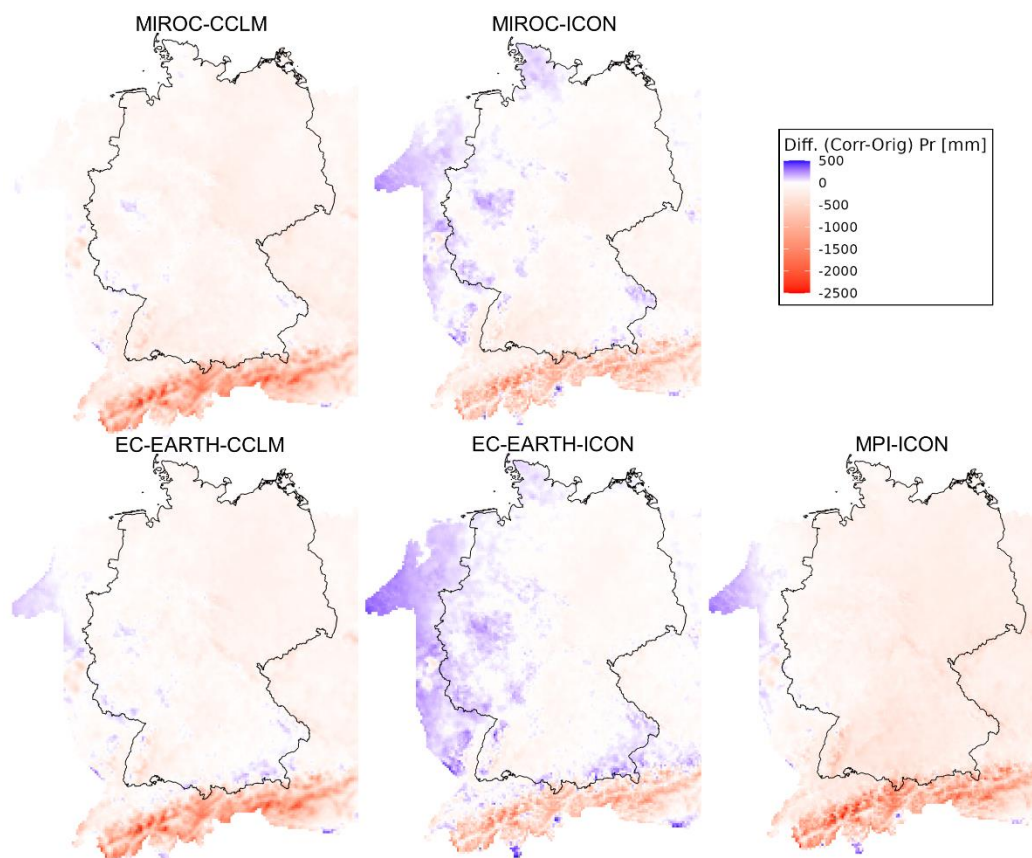


Figure A1: Mean bias of annual precipitation sums in the reference period (1961-1990) for the 5 model combinations.

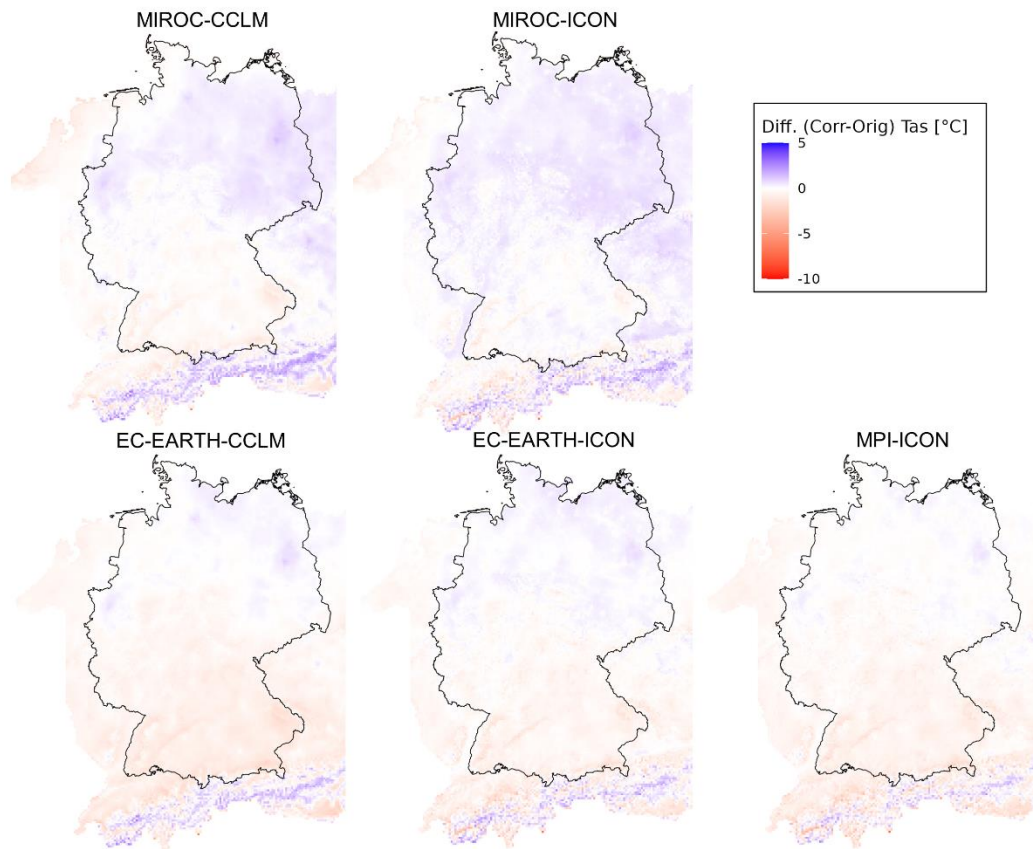


Figure A2: Mean bias of air temperature in the reference period (1961-1990) for the 5 model combinations.



Appendix B

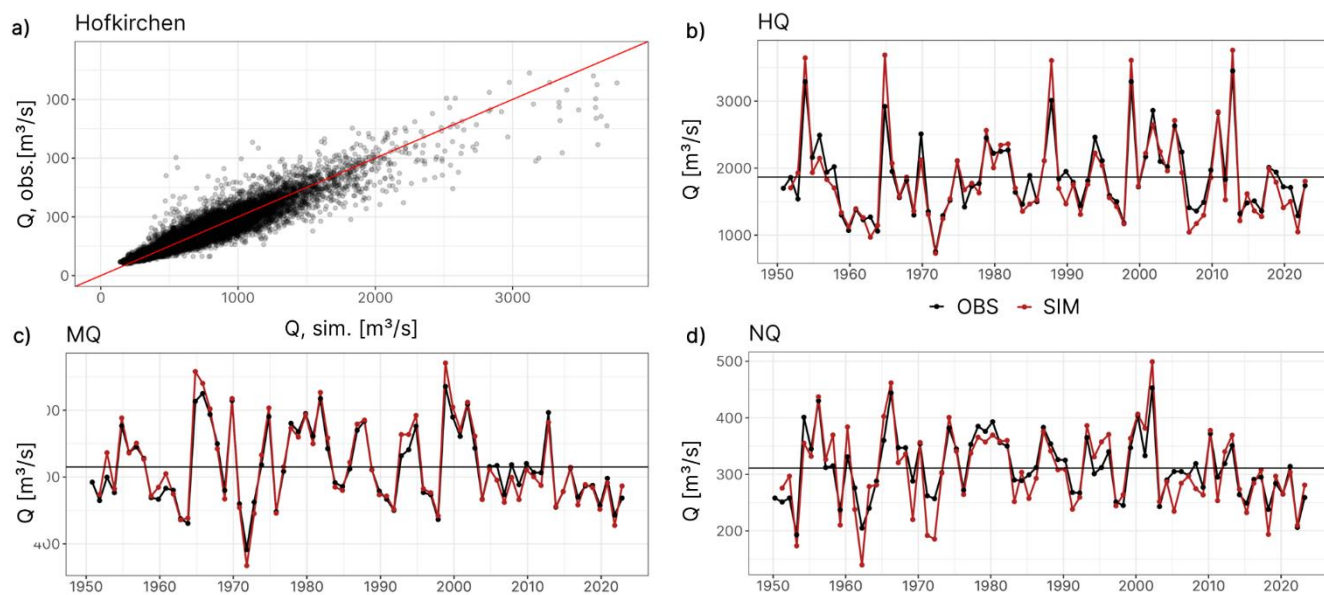


Figure B1: Simulated discharge (Q, sim) versus observed discharge (Q, obs) for station Hofkirchen/Danube in the period 1951–2023 (a). HQ (b), MQ (c) and NQ (d).

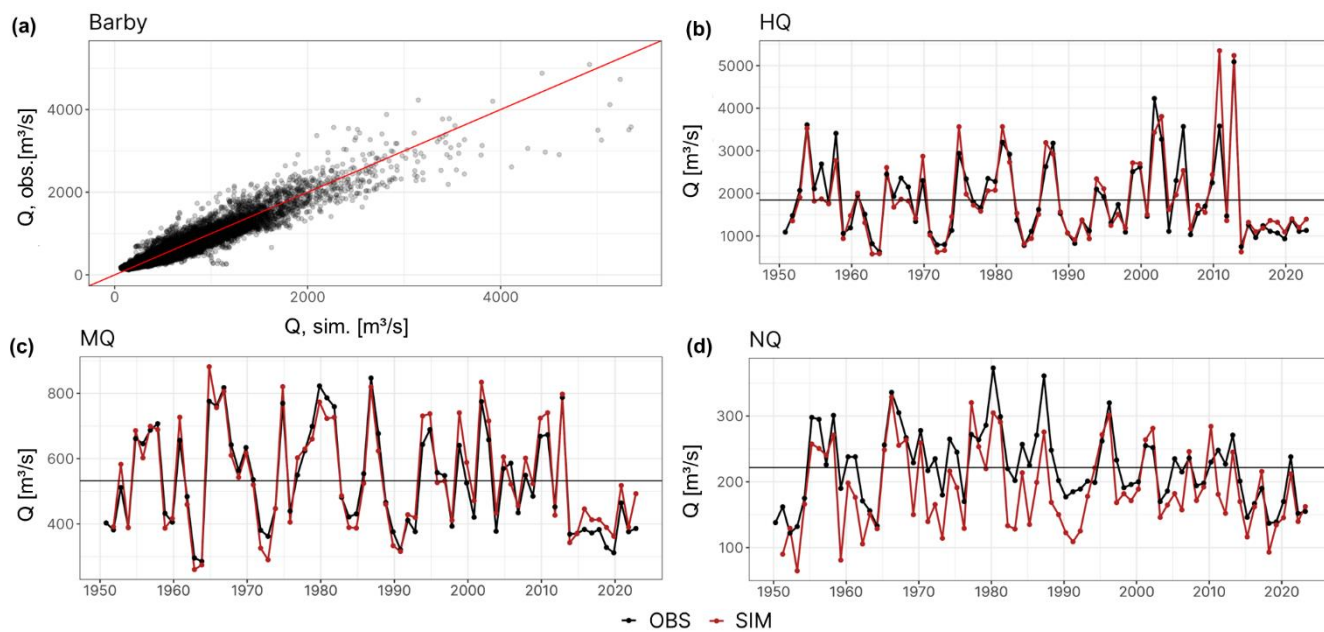


Figure B2: Simulated discharge (Q, sim) versus observed discharge (Q, obs) for station Barby/Elbe in the period 1951–2023 (a). HQ (b), MQ (c) and NQ (d).

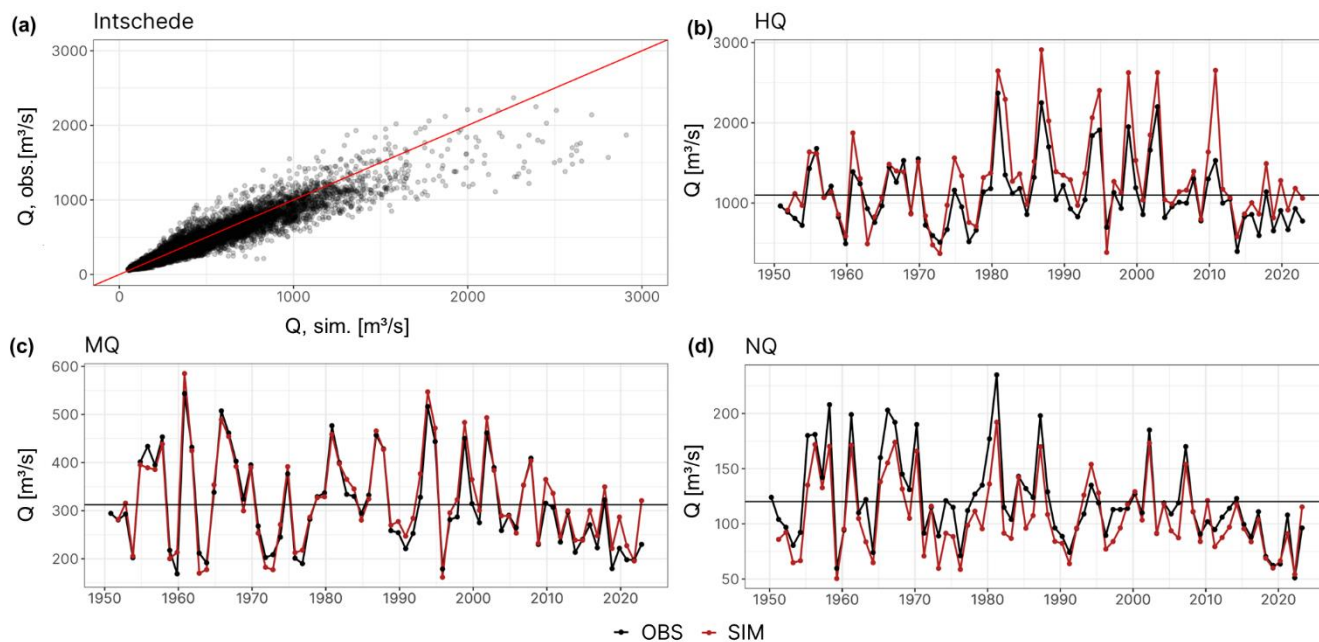


Figure B3: Simulated discharge (Q , sim) versus observed discharge (Q , obs) for station Intschede/Weser in the period 1951–2023 (a), HQ (b), MQ (c) and NQ (d).

365

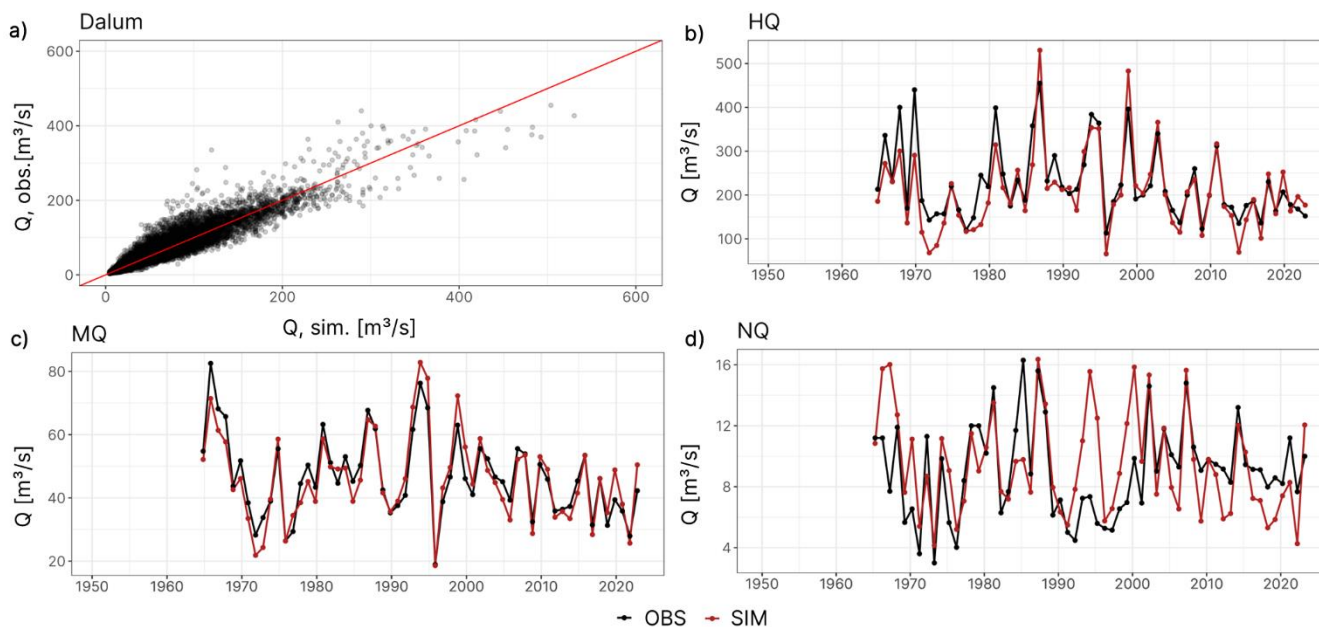


Figure B4: Simulated discharge (Q , sim) versus observed discharge (Q , obs) for station Dalum/Ems in the period 1965–2023 (a), HQ (b), MQ (c) and NQ (d).



Appendix C

370 **Table C1: Indicator MNQ of observed discharges for different period lengths at the stations Kaub/Rhine and Dalum/Ems.**

	Station Kaub/Rhine	Station Dalum/Ems
MNQ 30 years period 1961 – 1990	797.8 m ³ /s	9.3 m ³ /s
MNQ 29 years period 1962 – 1990	796.8 m ³ /s (0.1 % deviation)	9.3 m ³ /s (0 % deviation)
MNQ 28 years period 1962 – 1989	797.3 m ³ /s (0.06 % deviation)	9.4 m ³ /s (0.9 % deviation)

Appendix D

Table D1: Evaluated stations and associated catchment areas.

Station	River	River Basin District	Catchm. Area [km ²]
Achleiten	Danube	Danube	76653
Dillingen	Danube	Danube	11379
Donauwörth	Danube	Danube	15131
Hofkirchen	Danube	Danube	47518
Ingolstadt	Danube	Danube	20252
Kelheim	Danube	Danube	23031
Kelheimwinzer	Danube	Danube	26361
Oberndorf	Danube	Danube	26521
Pfelling	Danube	Danube	37775
Schwabelweis	Danube	Danube	35476
Passau Ingling	Inn	Danube	26040
Rosenheim o.d. Mangfallmünd	Inn	Danube	10154
Wasserburg	Inn	Danube	11960
Barby	Elbe	Elbe	94060
Dresden	Elbe	Elbe	53096
Magdeburg	Elbe	Elbe	94942
Neu Darchau	Elbe	Elbe	131950
Tangermünde	Elbe	Elbe	97780
Torgau Brücke	Elbe	Elbe	55211
Usti	Elbe	Elbe	48561
Wittenberg	Elbe	Elbe	61879
Wittenberge	Elbe	Elbe	123532
Calbe Grizehne	Saale	Elbe	23719



Dalum	Ems	Ems	4981
Versen	Ems	Ems	8411
Frankfurt	Main	Rhine	24764
Kleinheubach	Main	Rhine	21491
Raunheim	Main	Rhine	27142
Steinbach	Main	Rhine	17905
Trunstadt	Main	Rhine	12012
Würzburg	Main	Rhine	13996
Cochem	Moselle	Rhine	27088
Trier UP	Moselle	Rhine	23857
Rockenau-SKA	Neckar	Rhine	12710
Andernach	Rhine	Rhine	139549
Basel	Rhine	Rhine	35897
Bonn	Rhine	Rhine	140901
Düsseldorf	Rhine	Rhine	147680
Kaub	Rhine	Rhine	103729
Köln	Rhine	Rhine	144232
Lobith	Rhine	Rhine	159896
Mainz	Rhine	Rhine	98206
Maxau	Rhine	Rhine	50196
Rees	Rhine	Rhine	159300
Ruhrort	Rhine	Rhine	152895
Speyer	Rhine	Rhine	53131
Worms	Rhine	Rhine	68827
Bodenwerder	Weser	Weser	15924
Hann-Münden	Weser	Weser	12444
Intschede	Weser	Weser	37718
Liebenau	Weser	Weser	19910
Porta	Weser	Weser	19162
Vlotho	Weser	Weser	17618



375 Appendix E

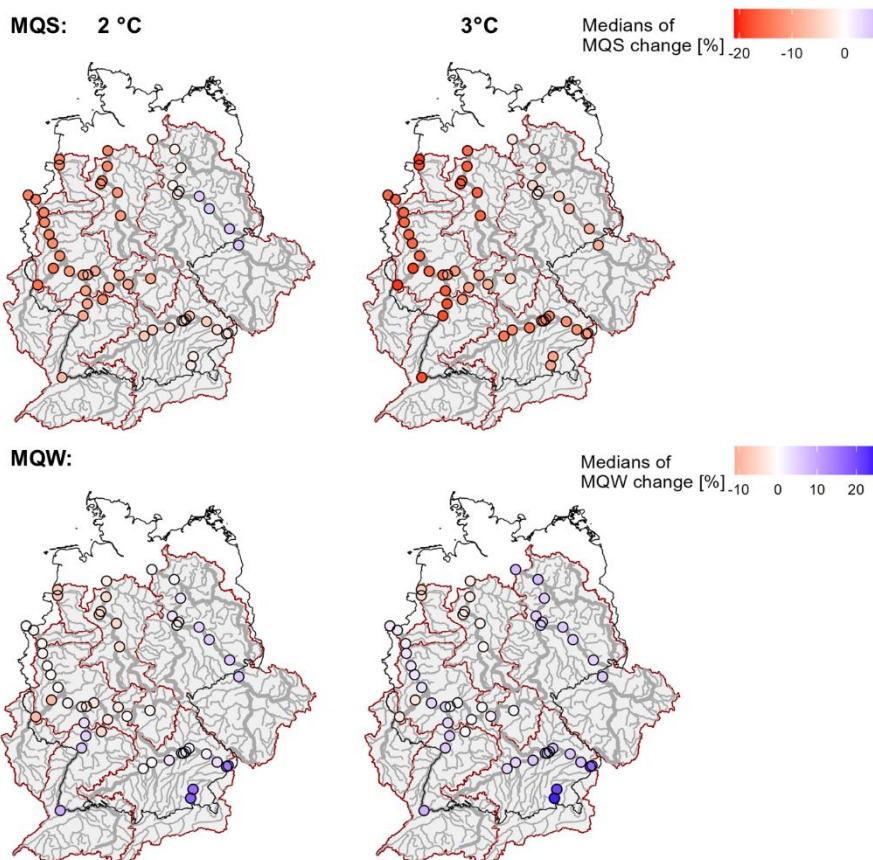


Figure E1: Indicators MQS (top, MQ in hydrological summer) and MQW (bottom, MQ in hydrological winter) for 53 catchments in the river basins of Rhine, Elbe, Danube, Weser and Ems. The colors represent the changes compared to the reference period for the NUKLEUS CMIP6 ensemble median.



380 Appendix F

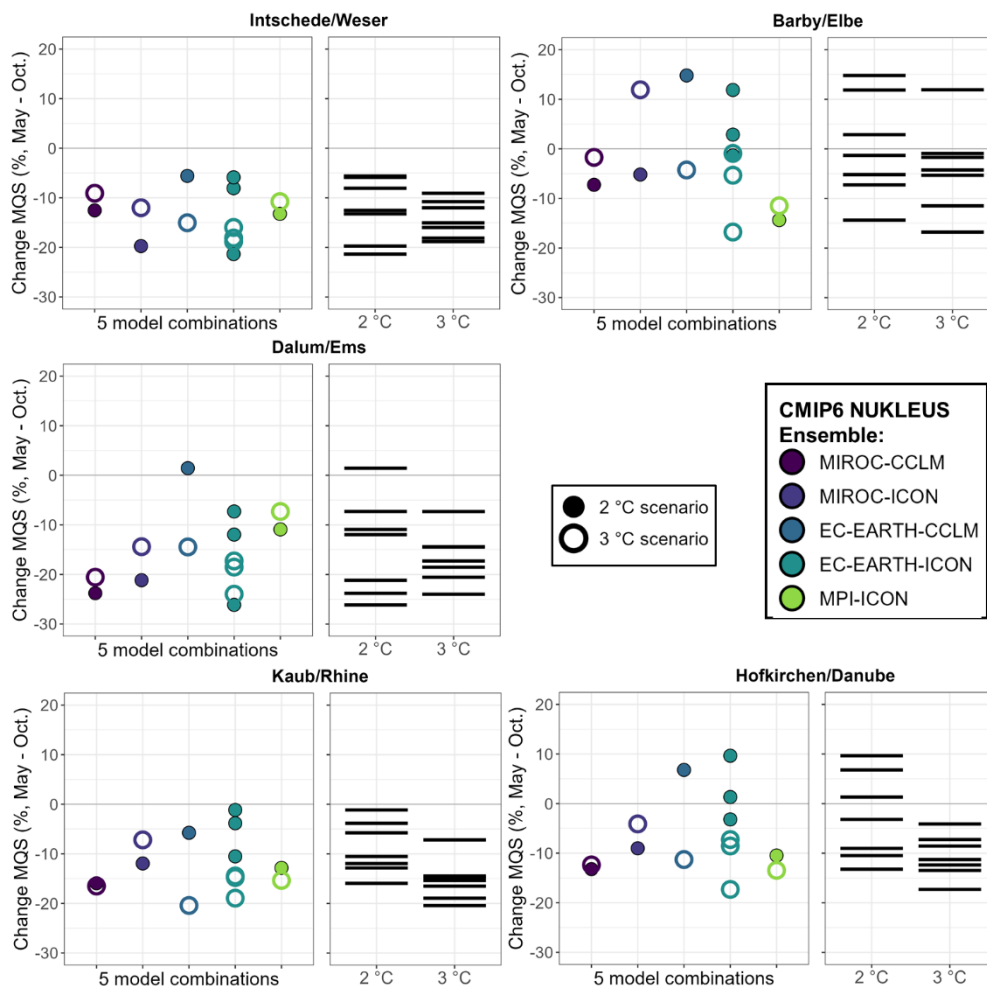
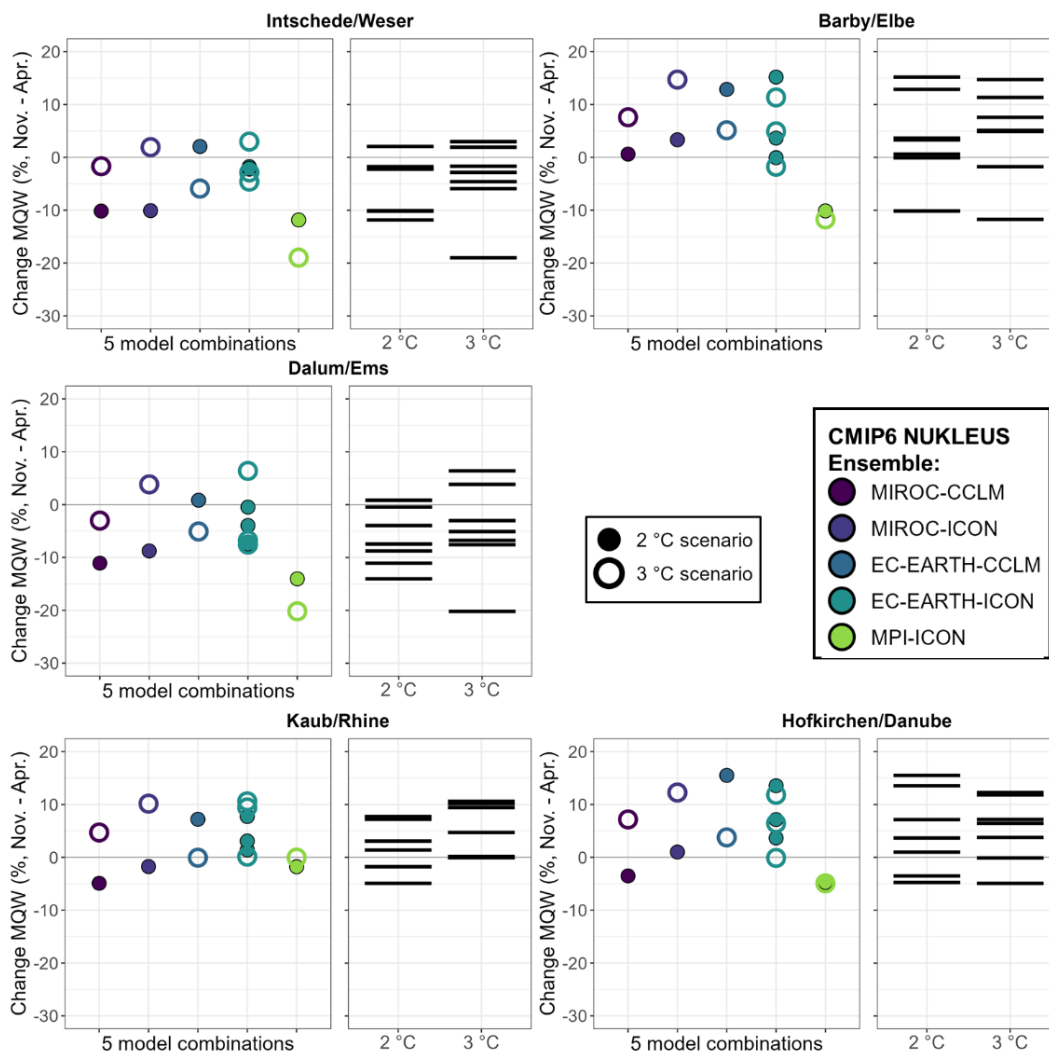


Figure F1: Change signal of MQS values (MQ for hydrological summer) for five model combinations in GWL 2 °C and 3 °C of the NUKLEUS CMIP6 ensemble for five indicator stations in German river basin districts.



385 **Figure F2:** Change signal of MQW values (MQ for hydrological winter) for five model combinations in GWL 2 °C and 3 °C of the NUKLEUS CMIP6 ensemble for five indicator stations in German river basin districts.

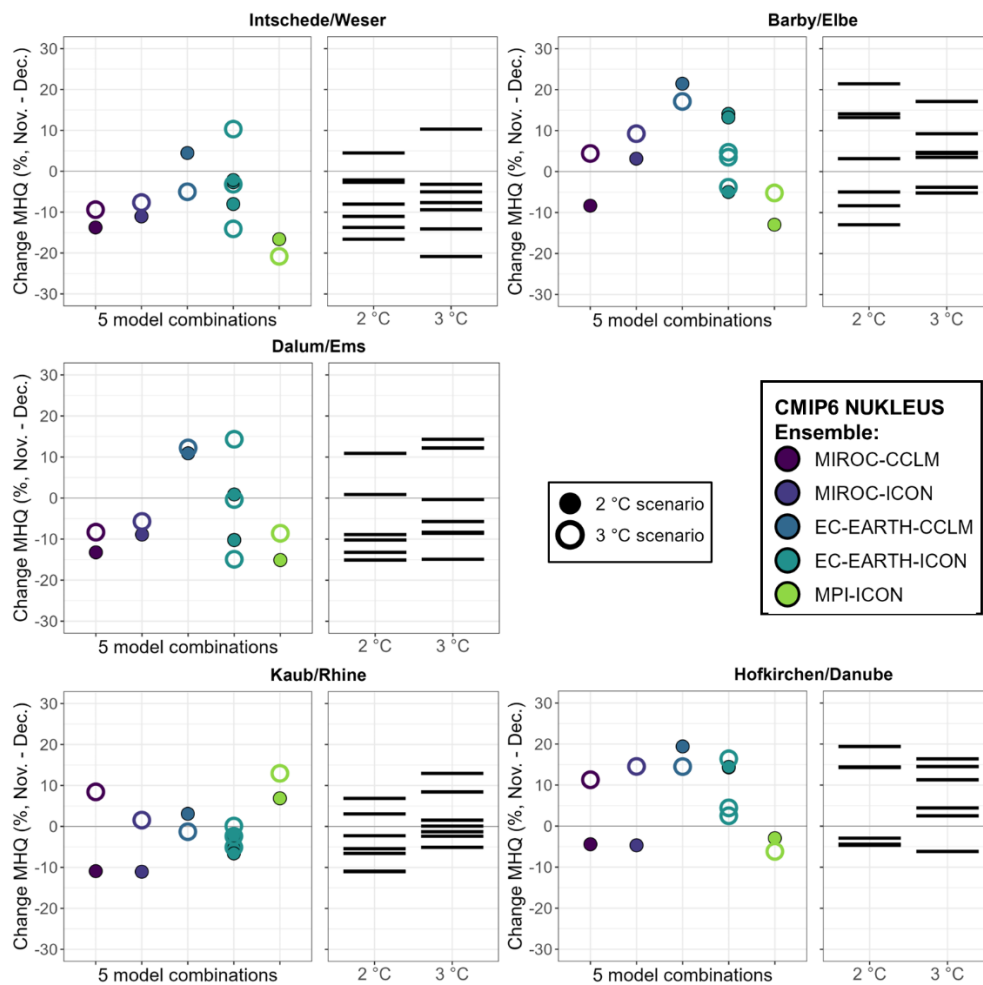
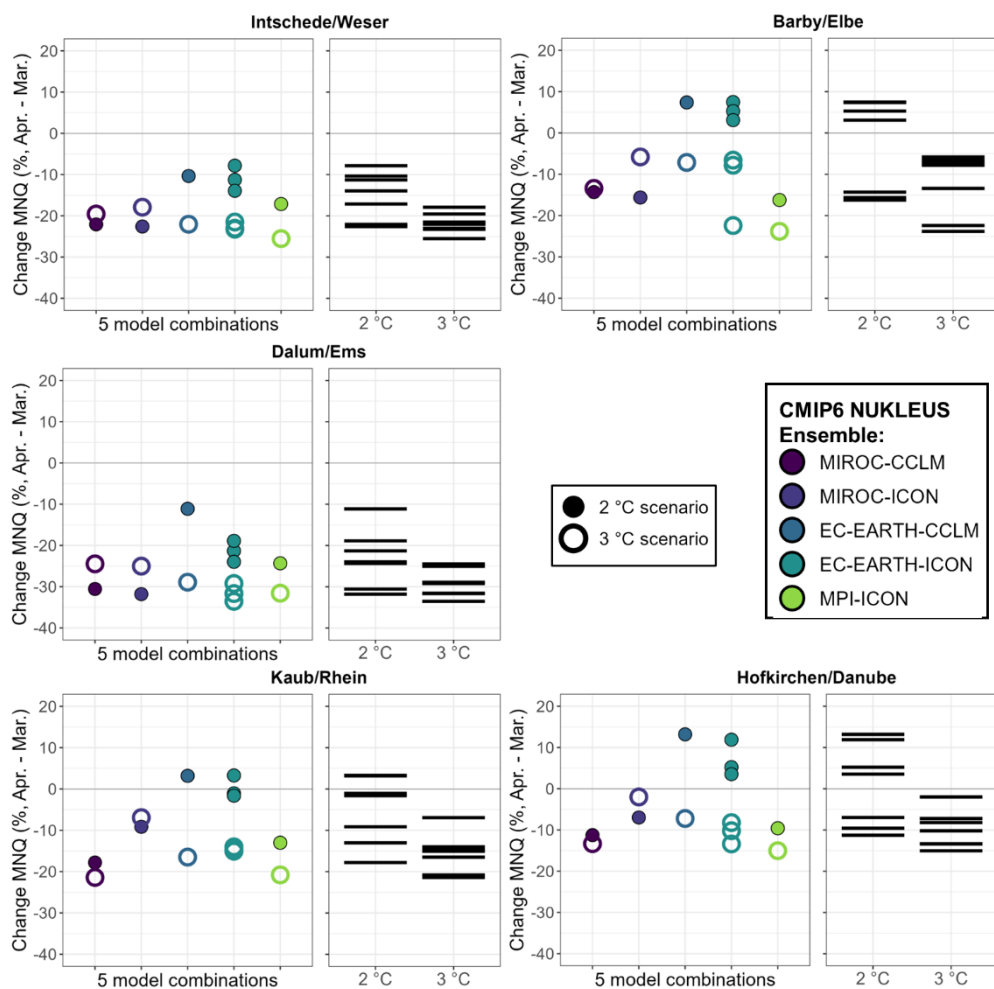


Figure F3: Multi-annual change signals for MHQ values of five model combinations and GWL 2 °C and 3 °C of the NUKLEUS CMIP6 ensemble for five indicator stations in German river basin districts relative to 1961-1990.



390

Figure F4: Multi-annual change signals for MNQ values of five model combinations and GWL 2 °C and 3 °C of the NUKLEUS CMIP6 ensemble for five indicator stations in German river basin districts relative to 1961-1990.

Data availability

The data that support the findings of this study are openly available on Zenodo at <https://doi.org/10.5281/zenodo.18298520> under the CC-BY-SA-4.0 licence.

395

Author contribution

JR conducted the analysis, developed the methods, investigation and visualization together with EN. EN gained access to the data and worked out the concept of the presented research, he was supervising the process. CF was responsible for the



hydrological model and software development. JR prepared the manuscript with contributions from all co-authors. CG
400 reviewed the manuscript.

Competing interests

The authors declare that they have no conflict of interest.

Acknowledgements

405 The works were conducted as the Federal Institute of Hydrology being associated partner of the funding measure “Regional information for action on climate change” (RegIKlim) of the German Federal Ministry of Education and Research (BMBF) in the R2K project.

References

- Anders, I., Stagl, J., Auer, I., Pavlik, D.: Climate Change in Central and Eastern Europe, in: Rannow, S., Neubert, M. (Eds.),
410 Managing Protected Areas in Central and Eastern Europe Under Climate Change, Advances in Global Change Research. Springer Netherlands, Dordrecht, 17–30. doi:10.1007/978-94-007-7960-0_2, 2014.
- Beier, C., Ziegler, K., Paeth, H., Pinto, J.P., Sieck, K., Bunttemeyer, L., Geyer, B., Xoplaki, E., Espitia, E., Braun, C., Ehmele, F., Feldmann, H., Kadow, C., Trachte, K.: A First Convection Permitting Multi-model Ensemble for Germany: Assessment of future changes in temperature and precipitation extremes. *Journal of Climate*, under review.
- 415 BMVI-Expertennetzwerk: Verkehr und Infrastruktur an Klimawandel und extreme Wetterereignisse anpassen, Ergebnisbericht des Themenfeldes 1 im BMVI-Expertennetzwerk für die Forschungsphase 2016 – 2019. Bundesministerium für Verkehr und digitale Infrastruktur (BMVI), Berlin, 2020.
- Boé, J., Terray, L., Habets, F., Martin, E.: Statistical and dynamical downscaling of the Seine basin climate for hydro-meteorological studies. *Intl Journal of Climatology* 27, 1643–1655. doi:10.1002/joc.1602, 2007.
- 420 Buitink, J., Tsiokanos, A., Geertsema, T., ten Velden, C., Bouaziz, L., Sperna Weiland, F.: Implications of the KNMI’23 climate scenarios for the discharge of the Rhine and Meuse (No. 11209265- 002- ZWS- 0003), Deltares, 2023.
- Bundesanstalt für Gewässerkunde: Informationsplattform UNDINE: <https://undine.bafg.de/>, last access:16 January 2026.
- Carbon Brief: CMIP6: The next generation of climate models explained [WWW Document]. Carbon Brief. URL <https://www.carbonbrief.org/cmip6-the-next-generation-of-climate-models-explained/>, 2020.



- 425 Carvalho, D., Rafael, S., Monteiro, A., Rodrigues, V., Lopes, M., Rocha, A.: How well have CMIP3, CMIP5 and CMIP6 future climate projections portrayed the recently observed warming. *Sci Rep* 12, 11983. doi:10.1038/s41598-022-16264-6, 2022.
- Chen, H., Sun, J., Lin, W., Xu, H.: Comparison of CMIP6 and CMIP5 models in simulating climate extremes. *Science Bulletin* 65, 1415–1418. doi:10.1016/j.scib.2020.05.015, 2020
- 430 Cusinato, E., Braun, C., Feldmann, H., Geyer, B., Keuler, K., Ludwig, P., Moemken, J., Sieck, K., Trachte, K., Frühe, B., Steger, C., Pinto, J.G.: Advancing regional to local climate knowledge: Insights from German NUKLEUS and UDAG Consortium Projects. doi:10.5194/egusphere-egu24-18143, 2025.
- Deman, J., Boé, J.: Future changes in runoff over western and central Europe: disentangling the hydrological behavior of CMIP6 models. *Earth Syst. Dynam.* 16, 1409–1426. doi:10.5194/esd-16-1409-2025, 2025.
- 435 Dobler, A., Feldmann, H., Meredith, E., Ulbrich, U.: Grenzen und Herausforderungen der regionalen Klimamodellierung, in: Brasseur, G.P., Jacob, D., Schuck-Zöller, S. (Eds.), *Klimawandel in Deutschland*. Springer Berlin Heidelberg, Berlin, Heidelberg, 47–56. doi:10.1007/978-3-662-66696-8_5, 2023.
- Eyring, V., Bony, S., Meehl, G.A., Senior, C.A., Stevens, B., Stouffer, R.J., Taylor, K.E.: Overview of the Coupled Model Intercomparison Project Phase 6 (CMIP6) experimental design and organization. *Geosci. Model Dev.* 9, 1937–1958. doi:10.5194/gmd-9-1937-2016, 2016.
- 440 Gudmundsson, L.: R package qmap: Statistical Transformations for Post-Processing Climate Model Output, 2016.
- Gupta, H.V., Kling, H., Yilmaz, K.K., Martinez, G.F.: Decomposition of the mean squared error and NSE performance criteria: Implications for improving hydrological modelling. *Journal of Hydrology* 377, 80–91. doi:10.1016/j.jhydrol.2009.08.003, 2009.
- 445 Gutiérrez, J.M., Jones, R.G., Narsima, G.T., Alves, L.M., Amjad, M., Gorodetskaya, I.V., Grose, M., Klutse, N.A.B., Krakovska, S., Li, J., Martinez-Castro, D., Mearns, L.O., Mernhild, S.H., Ngo-Duc, T., van den Hurk, B., Yoon, J.-H.: Atlas. In: *Climate Change 2021 – The Physical Science Basis: Working Group I Contribution to the Sixth Assessment Report of the Intergovernmental Panel on Climate Change*, 1st ed. Cambridge University Press. doi:10.1017/9781009157896, 2021.
- Haarsma, R.J., Roberts, M.J., Vidale, P.L., Senior, C.A., Bellucci, A., Bao, Q., Chang, P., Corti, S., Fučkar, N.S., Guemas, V., 450 Von Hardenberg, J., Hazeleger, W., Kodama, C., Koenigk, T., Leung, L.R., Lu, J., Luo, J.-J., Mao, J., Mizielinski, M.S., Mizuta, R., Nobre, P., Satoh, M., Scoccimarro, E., Semmler, T., Small, J., Von Storch, J.-S.: High Resolution Model Intercomparison Project (HighResMIP v1.0) for CMIP6. *Geosci. Model Dev.* 9, 4185–4208. doi:10.5194/gmd-9-4185-2016, 2016.
- Hundhausen, M., Fowler, H.J., Feldmann, H., Pinto, J.G.: Sub-hourly precipitation and rainstorm event profiles in a convection-permitting multi-GCM ensemble. *Weather and Climate Extremes* 48, 100764. doi:10.1016/j.wace.2025.100764, 2025.
- International Commission for the Hydrology of the Rhine basin: CHR - Gauge map: <https://www.chr-khr.org/en/gauges/map/785>, last access:16 December 2025.



- International Commission for the Protection of the Rhine: IKS-R-Niedrigwasserüberwachung am Rhein und in seinem Einzugsgebiet (No. 261), 2019.
- International Commission for the Protection of the Rhine: Klimawandelbedingte Abflussszenarien für das Rheineinzugsgebiet. Aktualisierung der Abflussszenarien im Rheineinzugsgebiet auf der Grundlage neuester Erkenntnisse über den Klimawandel (No. 297), Fachbericht, 2024.
- Kaspar, F., Mächel, H.: Beobachtung von Klima und Klimawandel in Mitteleuropa und Deutschland, in: Brasseur, G.P., Jacob, D., Schuck-Zöller, S. (Eds.), Klimawandel in Deutschland. Springer Berlin Heidelberg, Berlin, Heidelberg, pp. 19–30. doi:10.1007/978-3-662-66696-8_3, 2023.
- Klein, B. R package hydspatint: hydspatint - Downscaling of Meteorological Data for Hydrological Applications (unpublished), 2025.
- Kreienkamp, F., Lorenz, P., Geiger, T.: Statistically Downscaled CMIP6 Projections Show Stronger Warming for Germany. Atmosphere 11, 1245. doi:10.3390/atmos11111245, 2020.
- Kunstmann, H., Fröhle, P., Hattermann, F.F., Marx, A., Smiatek, G., Wanger, C.: Wasserhaushalt im Klimawandel, in: Brasseur, G.P., Jacob, D., Schuck-Zöller, S. (Eds.), Klimawandel in Deutschland. Springer Berlin Heidelberg, Berlin, Heidelberg, pp. 213–226. doi:10.1007/978-3-662-66696-8_16, 2023
- LARSIM-Entwicklergemeinschaft: Das Wasserhaushaltsmodell LARSIM - Modellgrundlagen und Anwendungsbeispiele. Hochwasserzentralen LUBW, BLfU, LfU RP, HLNUG, BAFU, 2024.
- Laux, P., Feldmann, D., Marra, F., Feldmann, H., Kunstmann, H., Trachte, K., Peleg, N.: Future precipitation extremes and urban flood risk assessment using a non-stationary and convection-permitting climate-hydrodynamic modeling framework. Journal of Hydrology 661, 133607. doi:10.1016/j.jhydrol.2025.133607, 2025.
- Lehner, B., Verdin, K., Jarvis, A.: New global hydrography derived from spaceborne elevation data. Eos, Transactions, 89(10): 93-94. Data available at <https://www.hydrosheds.org>, 2008.
- Lei, Y., Chen, J., Xiong, L.: A comparison of CMIP5 and CMIP6 climate model projections for hydrological impacts in China. Hydrology Research 54, 330–347. doi:10.2166/nh.2023.108, 2023.
- Manfred Bremicker: Das Wasserhaushaltsmodell LARSIM - Modellgrundlagen und Anwendungsbeispiele (No. Band 11), Freiburger Schriften zur Hydrologie. Institut für Hydrologie der Universität Freiburg i. Br., 2000.
- Meinshausen, M., Nicholls, Z.R.J., Lewis, J., Gidden, M.J., Vogel, E., Freund, M., Beyerle, U., Gessner, C., Nauels, A., Bauer, N., Canadell, J.G., Daniel, J.S., John, A., Krummel, P.B., Luderer, G., Meinshausen, N., Montzka, S.A., Rayner, P.J., Reimann, S., Smith, S.J., Van Den Berg, M., Velders, G.J.M., Vollmer, M.K., Wang, R.H.J.: The shared socio-economic pathway (SSP) greenhouse gas concentrations and their extensions to 2500. Geosci. Model Dev. 13, 3571–3605. doi:10.5194/gmd-13-3571-2020, 2020
- Nilson, E., Astor, B., Bergmann, L., Fischer, H., Fleischer, C., Haunert, G., Helms, M., Hillebrand, G., Höpp, S., Kikillus, A., Labadz, M., Mannfeld, M., Razafimaharo, C., Patzwahl, R., Rasquin, C., Rauthe, M., Riedel, A., Schröder, M., Schulz, D., Seiffert, R., Stachel, H., Wachler, B., Winkel, N.: Beiträge zu einer verkehrsträgerübergreifenden Klimawirkungsanalyse:



- Wasserstraßenspezifische Wirkungszusammenhänge, Schlussbericht des Schwerpunktthemas Schiffbarkeit und Wasserbeschaffenheit (SP-106) im Themenfeld 1 des BMVIExpertennetzwerks, 2020.
- 495 Nilson, E., Carambia, M., Krahe, P., Rachimow, C., Beersma, J., Deutsche Vereinigung für Wasserwirtschaft, Abwasser und Abfall (Eds.): Bias-Korrekturmodelle im Vergleich: Eine Bewertung im Kontext der hydrologischen Klimafolgenforschung, in: Nachhaltige Wasserwirtschaft durch Integration von Hydrologie, Hydraulik, Gewässerschutz und Ökonomie: Beiträge zum Tag der Hydrologie am 25./26. März 2010 an der Technischen Universität Braunschweig, Forum für Hydrologie und Wasserbewirtschaftung. Presented at the Tag der Hydrologie, DWA, Hennef, 2010.
- 500 Padulano, R., Gomez-Mogollon, L.A., Napolitano, L., Rianna, G.: Quantile-based bias-correction of extreme rainfall: Pros & cons of popular methods for climate signal preservation. *Journal of Hydrology* 653, 132814. doi:10.1016/j.jhydrol.2025.132814, 2025
- Palmer, T.E., Booth, B.B.B., McSweeney, C.F.: How does the CMIP6 ensemble change the picture for European climate projections? *Environ. Res. Lett.* 16, 094042. doi:10.1088/1748-9326/ac1ed9, 2021.
- 505 Raneesh, K., Thampi, S.G.: Bias Correction for RCM Predictions of Precipitation and Temperature in the Chaliyar River Basin. *J Climatol Weather Forecasting* 1. doi:10.4172/2332-2594.1000105, 2013.
- Rauthe, M., Brendel, C., Helms, M., Lohrengel, A.-F., Meine, L., Nilson, E., Norpoth, M., Rasquin, C., Rudolph, E., Schade, N.H., Deutschländer, T., Forbriger, M., Fleischer, C., Ganske, A., Herrmann, C., Kirsten, J., Möller, J., Seiffert, R.: Klimawirkungsanalyse des Bundesverkehrssystems im Kontext Hochwasser, Schlussbericht des Schwerpunktthemas
- 510 Hochwassergefahren (SP-103) im Themenfeld 1 des BMVI-Expertennetzwerks, 2020.
- Regenauer, J., Nilson, E.: Simulated discharges (by LARSIM-ME) of climate projections (NUKLEUS CMIP6 ensemble data), Zenodo [Data set], doi:10.5281/zenodo.18298520, 2026.
- Rottler, E., Bronstert, A., Bürger, G., Rakovec, O. Projected changes in Rhine River flood seasonality under global warming. *Hydrol. Earth Syst. Sci.* 25, 2353–2371. doi:10.5194/hess-25-2353-2021, 2021.
- 515 Schulzweida, U.: CDO User Guide. doi:10.5281/ZENODO.10020800, 2023.
- Sieck, K., Tiedje, B., Feldmann, H., Pinto, J.: NUKLEUS - User-relevant and applicable kilometer-scale climate information for Germany. doi:10.5194/egusphere-egu21-12137, 2021
- Sørland, S.L., Brogli, R., Pothapakula, P.K., Russo, E., Van De Walle, J., Ahrens, B., Anders, I., Bucchignani, E., Davin, E.L., Demory, M.-E., Dosio, A., Feldmann, H., Früh, B., Geyer, B., Keuler, K., Lee, D., Li, D., Van Lipzig, N.P.M., Min, S.-K.,
- 520 Panitz, H.-J., Rockel, B., Schär, C., Steger, C., Thiery, W.: COSMO-CLM regional climate simulations in the Coordinated Regional Climate Downscaling Experiment (CORDEX) framework: a review. *Geosci. Model Dev.* 14, 5125–5154. doi:10.5194/gmd-14-5125-2021, 2021.
- Teichmann, C., Bülow, K., Otto, J., Pfeifer, S., Rechid, D., Sieck, K., Jacob, D.: Avoiding Extremes: Benefits of Staying below +1.5 °C Compared to +2.0 °C and +3.0 °C Global Warming. *Atmosphere* 9, 115. doi:10.3390/atmos9040115, 2018.
- 525 The CMIP6 landscape: *Nat. Clim. Chang.* 9, 727–727. doi:10.1038/s41558-019-0599-1, 2019.



- Try, S., Tanaka, S., Tanaka, K., Sayama, T., Khujanazarov, T., Oeurng, C.: Comparison of CMIP5 and CMIP6 GCM performance for flood projections in the Mekong River Basin. *Journal of Hydrology: Regional Studies* 40, 101035. doi:10.1016/j.ejrh.2022.101035, 2022.
- 530 Van Pham, T., Steger, C., Rockel, B., Keuler, K., Kirchner, I., Mertens, M., Rieger, D., Zängl, G., Früh, B.: ICON in Climate Limited-area Mode (ICON release version 2.6.1): a new regional climate model. *Geosci. Model Dev.* 14, 985–1005. doi:10.5194/gmd-14-985-2021, 2021.
- Wang, A., Miao, Y., Kong, X., Wu, H.: Future Changes in Global Runoff and Runoff Coefficient From CMIP6 Multi-Model Simulation Under SSP1-2.6 and SSP5-8.5 Scenarios. *Earth's Future* 10, e2022EF002910. doi:10.1029/2022EF002910, 2022.
- 535 Wolf-Schumann, U., Lingemann, I., Hunger, M., Buchholz, O., Dorp, M., Elpers, C., Hellbach, C., Klein, B., Krahe, P., Krauter, G., Richter, K.-G., Vollmer, S.: LARSIM-ME: Aufbau eines Wasserhaushaltsmodells Mitteleuropa (DWA, Fachgemeinschaft Hydrologische Wissenschaften No. 33.13), Forum für Hydrologie und Wasserbewirtschaftung. DWA, Fachgemeinschaft Hydrologische Wissenschaften, 2013.
- Wu, Y., Miao, C., Slater, L., Fan, X., Chai, Y., Sorooshian, S.: Hydrological Projections under CMIP5 and CMIP6: Sources and Magnitudes of Uncertainty. *Bulletin of the American Meteorological Society* 105, E59–E74. doi:10.1175/BAMS-D-23-540 0104.1, 2024.
- Zängl, G., Reinert, D., Rípodas, P., Baldauf, M.: The ICON (ICOsahedral Nonhydrostatic) modelling framework of DWD and MPI-M: Description of the nonhydrostatic dynamical core. *Quart J Royal Meteor Soc* 141, 563–579. doi:10.1002/qj.2378, 2015.